Boundary-value problem for plasma centrifuge at arbitrary magnetic Reynolds numbers*

H. E. Wilhelm and S. H. Hong
Department of Electrical Engineering, Colorado State University, Fort Collins, Colorado 80523
(Received 12 October 1976)

We solve in closed form the boundary-value problem for the partial differential equations which describe the (azimuthal) rotation velocity and induced magnetic fields in a cylindrical plasma centrifuge with ring electrodes of different radii and an external, axial magnetic field. The electric field, current density, and velocity distributions are discussed in terms of the Hartmann number H and the magnetic Reynolds number R. For small Hall coefficients, $\omega\tau \ll 1$, the induced magnetic field does not affect the plasma rotation. As a result of the Lorentz forces, the plasma rotates with speeds as high as 10^5 cm/sec around its axis of symmetry at typical conditions, so that the lighter (heavier) ion and atom components are enriched at (off) the center of the discharge cylinder.

I. INTRODUCTION

In principle, electromagnetic forces allow plasmas to be rotated up to relativistic speeds. Theta pinch experiments show that the plasma rotates during the discharge pulse at such high speeds that the energy distribution of the emitted neutrons is shifted.[1] From the theoretical point of view, the basic mechanism for plasma rotation by means of crossed electric and magnetic fields and Lorentz forces in rarefied[1-15] and dense[16-19] plasmas is understood qualitatively. Experimental evidence on isotope separation in rotating plasmas has been reported, e.g., by Bonnevier,[10,11] Guilloud,[20] Heller and Simon,[21] James and Simpson,[22] and Ban and Sekiguchi.[23,24] Exact solutions for the boundary-value problems describing plasma centrifuge systems are not known, either for collision-dominated[25,26] or for collisionless[2-4] plasmas.

A simple model for an electrical discharge centrifuge with an axial, external magnetic field $\vec{B}_0$ is shown in Fig. 1. This plasma centrifuge employs electrodes of different radii R_+ and R_- ($R_+ \gg R_-$) in the end plates $z = \pm c$ of an electrically isolating discharge chamber of radius R_0 so that the field lines of the current density $\vec{j}$ and of the external axial magnetic field $\vec{B}_0$ cross under a nonvanishing angle (except at the chamber axis). The resultant Lorentz force $\vec{j} \times \vec{B}_0$ rotates the discharge around its axis of symmetry. In steady state, the magnetic body forces in the azimuthal direction are balanced by the viscous forces (boundary layers at the chamber walls). As opposed to a centrifuge with radial electric current flow between inner and outer cylinder electrodes, the centrifuge scheme in Fig. 1 avoids the boundary layer and losses at the inner cylinder surface. In the following, the boundary-value problem for this centrifuge is solved in closed form based on the magnetogasdynamic equations for dense isotope plasmas with negligible Hall effect, i.e., $\omega\tau \ll 1$ ($\omega = eB/m$ and τ are the gyration frequency and collision time of the electrons).

II. BOUNDARY-VALUE PROBLEM

The plasma centrifuge model under consideration is depicted schematically in Fig. 1. The plasma is sustained by a discharge current I, which enters the centrifuge chamber of radius R_0 through a ring anode of radius R_+ in the anode plane $z = +c$ and leaves it through a ring cathode of radius R_- in the cathode plane $z = -c$. Accordingly,

$$2\pi \int_0^{R_0} j_z(r,z) r\, dr = I \int_0^{R_0} \delta(r - R_\pm)\, dr = I\,,$$

[$\delta(r - R_\pm)$ is the Dirac function] for the axial current density j_z in any plane $-c \le z \le +c$. The external magnetic field is axial and homogeneous: $\vec{B}_0 = (0, 0, B_0)$. In view of the symmetry of the system with respect to the axis $r = 0$, the plasma flow field is azimuthal, $\vec{V} = (0, V_\theta(r,z), 0)$, so that $\nabla \cdot \vec{V} = 0$, i.e., the plasma flow is incompressible. For negligible Hall effect ($\omega\tau \ll 1$), $j_\theta = 0$ and $\nabla \times \vec{B}$

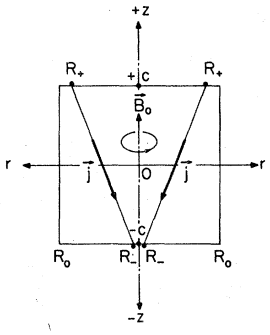

FIG. 1. Scheme of plasma centrifuge of radius R_0 and height $2c$ with cathode (R_-), anode (R_+), and axial magnetic field $\vec{B}_0$ ($R_+ \gg R_-$).

$= \mu_0(j_r, 0, j_z)$ in accordance with Maxwell's equation for the magnetic induction $\vec{B}$. Hence, $B_r = 0$ and $B_z = 0$ because of the homogeneous boundary conditions for B_r and B_z. However, $B_\theta(r,z) \neq 0$, since

$$B_\theta(r,z)_{r=R_0} = \mu_0 I/2\pi R_0, \quad -c \leq z \leq +c,$$

$$\frac{1}{r}\frac{\partial}{\partial r}[rB_\theta(r,z)]_{z=\pm c} = \frac{\mu_0 I}{2\pi}\frac{\delta(r-R_\pm)}{r}, \quad 0 \leq r \leq R_0.$$

Since the induced magnetic field (B_θ) is azimuthal, the induced electric field (E_r) is due to the rotation (V_θ) of the plasma across the external magnetic field (B_0). The pressure distribution $p(r,z)$ in the rotating plasma is determined by the r and z components of the magnetogasdynamic equation of motion[27] (ρ_P = plasma density),

$$-\rho_P\frac{V_\theta^2}{r} = -\frac{\partial p}{\partial r} - j_z B_\theta, \quad 0 = -\frac{\partial p}{\partial z} + j_r B_\theta,$$

where

$$\frac{1}{r}\frac{\partial}{\partial r}(rB_\theta) = \mu_0 j_z, \quad -\frac{\partial B_\theta}{\partial z} = \mu_0 j_r.$$

The current density $\vec{j}(r,z)$ and pressure $p(r,z)$ fields are readily determined from the magnetic field $\vec{B} = (0, B_\theta, B_0)$ and the velocity field $\vec{V} = (0, V_\theta, 0)$, whereas the electric field is given by Ohm's law, $\vec{E} = -\vec{V}\times\vec{B} + \vec{j}/\sigma$. The fields $V_\theta(r,z)$ and $B_\theta(r,z)$ are described by the θ components of the magnetogasdynamic equation of motion and the magnetic induction equation, respectively.[27]

For physical and mathematical reasons, it is suitable to formulate the boundary-value problem for the coupled plasma fields $V_\theta(r,z)$ and $B_\theta(r,z)$ in dimensionless form by introducing the dimensionless independent and dependent variables

$$\rho = r/R_0, \quad 0 \leq \rho \leq 1, \tag{1}$$

$$\zeta = z/c, \quad -1 \leq \zeta \leq +1, \tag{2}$$

and

$$V(\rho,\zeta) = V_\theta(r,z)/V_0, \quad B(\rho,\zeta) = B_\theta(r,z)/B_0, \tag{3}$$

where the reference value V_0 is defined as

$$V_0 \equiv I/2\pi R_0 B_0 \sigma c. \tag{4}$$

In the dimensionless formulation, the boundary-value problem for the azimuthal velocity $V(\rho,\zeta)$ and azimuthal induction $B(\rho,\zeta)$ fields assumes the form

$$\frac{1}{\rho}\frac{\partial}{\partial\rho}\left(\rho\frac{\partial V}{\partial\rho}\right) - \frac{V}{\rho^2} + N^{-2}\frac{\partial^2 V}{\partial\zeta^2} = -\frac{H^2}{R}\frac{\partial B}{\partial\zeta}, \tag{5}$$

$$\frac{1}{\rho}\frac{\partial}{\partial\rho}\left(\rho\frac{\partial B}{\partial\rho}\right) - \frac{B}{\rho^2} + N^{-2}\frac{\partial^2 B}{\partial\zeta^2} = -\frac{R}{N^2}\frac{\partial V}{\partial\zeta}, \tag{6}$$

where

$$V(\rho,\zeta)_{\rho=1} = 0, \quad -1 \leq \zeta \leq +1, \tag{7}$$

$$V(\rho,\zeta)_{\zeta=\pm1} = 0, \quad 0 \leq \rho \leq 1, \tag{8}$$

and

$$B(\rho,\zeta)_{\rho=1} = R, \quad -1 \leq \zeta \leq +1, \tag{9}$$

$$\frac{1}{\rho}\frac{\partial}{\partial\rho}[\rho B(\rho,\zeta)]_{\zeta=\pm1} = \frac{R\delta(\rho-\rho_\pm)}{\rho}, \quad 0 \leq \rho \leq 1, \tag{10}$$

with

$$H \equiv (\sigma/\mu)^{1/2} B_0 R_0, N \equiv c/R_0, \quad R \equiv \mu_0 I/2\pi R_0 B_0 \equiv \mu_0 \sigma V_0 c \gtrless 0. \tag{11}$$

The Hartmann number H (μ is the plasma viscosity), N, and the magnetic Reynolds number R characterize the ratio of Lorentz to viscous forces, the geometry of the centrifuge, and the intensity ratio of the induced and external magnetic fields, respectively. Equations (7), (8) and (9), (10) are the homogeneous and inhomogeneous boundary conditions for the fields $V(\rho,\zeta)$ and $B(\rho,\zeta)$, respectively. The linear statement,

$$B(\rho,\zeta) = R\rho + \Psi(\rho,\zeta), \tag{12}$$

reduces the Eqs. (6), (9), and (10) for $B(\rho,\zeta)$ to equations with a homogeneous boundary condition (14) for $\Psi(\rho,\zeta)$

$$\frac{1}{\rho}\frac{\partial}{\partial\rho}\left(\rho\frac{\partial\Psi}{\partial\rho}\right) - \frac{\Psi}{\rho^2} + N^{-2}\frac{\partial^2\Psi}{\partial\zeta^2} = -\frac{R}{N^2}\frac{\partial V}{\partial\zeta}, \tag{13}$$

where

$$\Psi(\rho,\zeta)_{\rho=1} = 0, \quad -1 \leq \zeta \leq +1, \tag{14}$$

$$\frac{1}{\rho}\frac{\partial}{\partial\rho}[\rho\Psi(\rho,\zeta)]_{\zeta=\pm1} = R\left(\frac{\delta(\rho-\rho_\pm)}{\rho} - 2\right), \quad 0 \leq \rho \leq 1. \tag{15}$$

Introducing Bessel's function $J_1(k_n\rho)$ of first order, partial solutions of the coupled inhomogeneous Eqs. (5) and (13) are sought in the form,

$$V_n(\rho,\zeta) = J_1(k_n\rho) f_n(\zeta), \tag{16}$$

$$\Psi_n(\rho,\zeta) = J_1(k_n\rho) g_n(\zeta), \tag{17}$$

where the eigenvalues $k_n > 0$ are determined by the homogeneous boundary conditions (7) and (14) as the real roots of the transcendental equation,

$$J_1(k_n) = 0, \quad n = 1, 2, 3, \ldots. \tag{18}$$

Thus, the general solution of the coupled Eqs. (5) and (13) obtains by linear superposition as the Fourier-Bessel series[28]

$$V(\rho,\zeta) = \sum_{n=1}^{\infty} J_1(k_n\rho) f_n(\zeta), \tag{19}$$

$$\Psi(\rho,\zeta) = \sum_{n=1}^{\infty} J_1(k_n\rho) g_n(\zeta). \tag{20}$$

Substitution of Eqs. (16) and (17) into Eqs. (5) and (13) yields ordinary coupled differential equations

of second order for $f_n(\zeta)$ and $g_n(\zeta)$:

$$f_n'' - k_n^2 N^2 f_n = -H^2 N^2 R^{-1} g_n', \tag{21}$$

$$g_n'' - k_n^2 N^2 g_n = -R f_n'. \tag{22}$$

By elimination, Eqs. (21) and (22) are reduced to decoupled differential equations of fourth order,

$$f_n'''' - (2k_n^2 + H^2) N^2 f_n'' + k_n^4 N^4 f_n = 0, \tag{23}$$

$$g_n'''' - (2k_n^2 + H^2) N^2 g_n'' + k_n^4 N^4 g_n = 0, \tag{24}$$

with

$$f_n(\zeta)_{\zeta = \pm 1} = 0, \tag{25}$$

$$g_n(\zeta)_{\zeta = \pm 1} = 2R k_n^{-1} J_0(k_n \rho_\pm) / J_0^2(k_n), \tag{26}$$

as boundary conditions, by Eqs. (8) and (15), respectively. In deriving Eq. (26), the Dirac function in Eq. (15) has been expanded in the Fourier-Dini series,[28]

$$\frac{\delta(\rho - \rho_\pm)}{\rho} = 2 + 2 \sum_{n=1}^{\infty} \frac{J_0(k_n \rho_\pm)}{J_0^2(k_n)} J_0(k_n \rho). \tag{27}$$

In addition to Eqs. (25) and (26), $f_n(\zeta)$ and $g_n(\zeta)$ have to satisfy also the coupled Eqs. (21) and (22). With the four real roots of Eqs. (23) and (24) [$f_n, g_n \propto e^{\omega \zeta}$],

$$\omega_{1n} = \omega_n^+, \quad \omega_{2n} = \omega_n^-, \quad \omega_{3n} = -\omega_n^+, \quad \omega_{4n} = -\omega_n^-, \tag{28}$$

where

$$\omega_n^\pm \equiv 2^{-1/2} N \{(2k_n^2 + H^2) \pm [(2k_n^2 + H^2)^2 - 4k_n^4]^{1/2}\}^{1/2}, \tag{29}$$

the general solutions for $f_n(\zeta)$ and $g_n(\zeta)$ of Eqs. (23) and (24) can be written as

$$f_n(\zeta) = A_n^+ \frac{\sinh \omega_n^+ \zeta}{\sinh \omega_n^+} + B_n^+ \frac{\cosh \omega_n^+ \zeta}{\cosh \omega_n^+} + A_n^- \frac{\sinh \omega_n^- \zeta}{\sinh \omega_n^-} + B_n^- \frac{\cosh \omega_n^- \zeta}{\cosh \omega_n^-}, \tag{30}$$

$$g_n(\zeta) = C_n^+ \frac{\sinh \omega_n^+ \zeta}{\sinh \omega_n^+} + D_n^+ \frac{\cosh \omega_n^+ \zeta}{\cosh \omega_n^+} + C_n^- \frac{\sinh \omega_n^- \zeta}{\sinh \omega_n^-} + D_n^- \frac{\cosh \omega_n^- \zeta}{\cosh \omega_n^-}. \tag{31}$$

Only four of the eight integration constants $A_n^\pm, \ldots D_n^\pm$ are independent. Substitution of Eqs. (30) and (31) into Eq. (21) and Eq. (22) yields

$$A_n^\pm [(\omega_n^\pm)^2 - k_n^2 N^2] / \omega_n^\pm = -H^2 N^2 R^{-1} \tanh \omega_n^\pm D_n^\pm, \tag{32}$$

$$B_n^\pm [(\omega_n^\pm)^2 - k_n^2 N^2] / \omega_n^\pm = -H^2 N^2 R^{-1} \coth \omega_n^\pm C_n^\pm, \tag{33}$$

and

$$C_n^\pm [(\omega_n^\pm)^2 - k_n^2 N^2] / \omega_n^\pm = -R \tanh \omega_n^\pm B_n^\pm, \tag{34}$$

$$D_n^\pm [(\omega_n^\pm)^2 - k_n^2 N^2] / \omega_n^\pm = -R \coth \omega_n^\pm A_n^\pm, \tag{35}$$

respectively. The coefficient determinant of Eqs. (32) and (35) or Eqs. (33) and (34) vanishes (condition for existence of nontrivial solution),

$$\Delta^\pm \equiv [(\omega_n^\pm)^2 - k_n^2 N^2]^2 - H^2 N^2 (\omega_n^\pm)^2 = 0, \tag{36}$$

in agreement with Eq. (29). From the latter or Eq. (36) one deduces the relations,

$$[(\omega_n^\pm)^2 - k_n^2 N^2] / \omega_n^\pm = \pm NH, \tag{37}$$

which simplify the left sides of Eqs. (32) and (35).

Application of the boundary conditions (35) to Eq. (30) shows that

$$-A_n^- = +A_n^+ \equiv A_n, \quad -B_n^- = +B_n^+ \equiv B_n. \tag{38}$$

Substitution of Eq. (38) into Eqs. (30) and (31) gives

$$f_n(\zeta) = A_n \left(\frac{\sinh \omega_n^+ \zeta}{\sinh \omega_n^+} - \frac{\sinh \omega_n^- \zeta}{\sinh \omega_n^-} \right) + B_n \left(\frac{\cosh \omega_n^+ \zeta}{\cosh \omega_n^+} - \frac{\cosh \omega_n^- \zeta}{\cosh \omega_n^-} \right) \tag{39}$$

and

$$g_n(\zeta) = -A_n \frac{R}{NH} \left(\frac{\cosh \omega_n^+ \zeta}{\sinh \omega_n^+} + \frac{\cosh \omega_n^- \zeta}{\sinh \omega_n^-} \right) - B_n \frac{R}{NH} \left(\frac{\sinh \omega_n^+ \zeta}{\cosh \omega_n^+} + \frac{\sinh \omega_n^- \zeta}{\cosh \omega_n^-} \right), \tag{40}$$

the latter under consideration of Eqs. (34), (35) and (37). Application of the boundary conditions (26) to Eq. (40) yields, upon elimination,

$$A_n = -\frac{NH}{k_n} \frac{J_0(k_n \rho_-) + J_0(k_n \rho_+)}{(\coth \omega_n^+ + \coth \omega_n^-) J_0^2(k_n)}, \tag{41}$$

$$B_n = +\frac{NH}{k_n} \frac{J_0(k_n \rho_-) - J_0(k_n \rho_+)}{(\tanh \omega_n^+ + \tanh \omega_n^-) J_0^2(k_n)}. \tag{42}$$

By combining Eqs. (39)–(42), we obtain the solutions for $f_n(\zeta)$ and $g_n(\zeta)$ in final form:

$$\frac{f_n(\zeta)}{NH} = -\frac{J_0(k_n \rho_-) + J_0(k_n \rho_+)}{(\coth \omega_n^+ + \coth \omega_n^-) k_n J_0^2(k_n)} \left(\frac{\sinh \omega_n^+ \zeta}{\sinh \omega_n^+} - \frac{\sinh \omega_n^- \zeta}{\sinh \omega_n^-} \right) + \frac{J_0(k_n \rho_-) - J_0(k_n \rho_+)}{(\tanh \omega_n^+ + \tanh \omega_n^-) k_n J_0^2(k_n)} \left(\frac{\cosh \omega_n^+ \zeta}{\cosh \omega_n^+} - \frac{\cosh \omega_n^- \zeta}{\cosh \omega_n^-} \right), \tag{43}$$

$$\frac{g_n(\zeta)}{R} = +\frac{J_0(k_n \rho_-) + J_0(k_n \rho_+)}{(\coth \omega_n^+ + \coth \omega_n^-) k_n J_0^2(k_n)} \left(\frac{\cosh \omega_n^+ \zeta}{\sinh \omega_n^+} + \frac{\cosh \omega_n^- \zeta}{\sinh \omega_n^-} \right) - \frac{J_0(k_n \rho_-) - J_0(k_n \rho_+)}{(\tanh \omega_n^+ + \tanh \omega_n^-) k_n J_0^2(k_n)} \left(\frac{\sinh \omega_n^+ \zeta}{\cosh \omega_n^+} + \frac{\sinh \omega_n^- \zeta}{\cosh \omega_n^-} \right). \tag{44}$$

Below, also the ζ derivative of $g_n(\zeta)$ is required, which is given by

$$\frac{g_n'(\zeta)}{R} = +\frac{J_0(k_n\rho_-)+J_0(k_n\rho_+)}{(\coth\omega_n^+ + \coth\omega_n^-)k_nJ_0^2(k_n)}\left(\omega_n^+\frac{\sinh\omega_n^+\zeta}{\sinh\omega_n^+}+\omega_n^-\frac{\sinh\omega_n^-\zeta}{\sinh\omega_n^-}\right)$$
$$-\frac{J_0(K_n\rho_-)-J_0(k_n\rho_+)}{(\tanh\omega_n^+ + \tanh\omega_n^-)k_nJ_0^2(k_n)}\left(\omega_n^+\frac{\cosh\omega_n^+\zeta}{\cosh\omega_n^+}+\omega_n^-\frac{\cosh\omega_n^-\zeta}{\cosh\omega_n^-}\right). \quad (45)$$

In terms of $f_n(\zeta)$, $g_n(\zeta)$, and $g_n'(\zeta)$, the solutions for the dimensionless fields $\vec{V}=(0,V,0)$, $\vec{B}=(0,B,1)$, $\vec{J}=(J_\rho,0,J_\zeta)$, and $\vec{E}=(E_\rho,0,E_\zeta)$ of the plasma centrifuge are by Eqs. (12), (19), and (20)

$$V(\rho,\zeta)=\sum_{n=1}^{\infty}J_1(k_n\rho)f_n(\zeta), \quad (46)$$

$$B(\rho,\zeta)=R\rho+\sum_{n=1}^{\infty}J_1(k_n\rho)g_n(\zeta), \quad (47)$$

$$J_\rho(\rho,\zeta)=-R^{-1}N^{-1}\sum_{n=1}^{\infty}J_1(k_n\rho)g_n'(\zeta), \quad (48)$$

$$J_\zeta(\rho,\zeta)=2+R^{-1}\sum_{n=1}^{\infty}k_nJ_0(k_n\rho)g_n(\zeta), \quad (49)$$

$$E_\rho(\rho,\zeta)=-V(\rho,\zeta)+NJ_\rho(\rho,\zeta),\quad E_\zeta(\rho,\zeta)=NJ_\zeta(\rho,\zeta). \quad (50)$$

The reference values V_0 and B_0 for $V(\rho,\zeta)$ and $B(\rho,\zeta)$ are defined in Eq. (4). The dimensionless fields $J_{\rho,\zeta}(\rho,\zeta)$ and $E_{\rho,\zeta}(\rho,\zeta)$ are normalized with respect to

$$j_0=I/2\pi R_0^2,\quad E_0\equiv V_0B_0=I/2\pi R_0\sigma c. \quad (51)$$

If the cathode is in the plane $z=-c$ ($\zeta=-1$) and the anode is in the plane $z=+c$ ($\zeta=+1$), then the reference fields V_0, j_0, and E_0 [Eqs. (4),(51)] are negative, since $I<0$. The results are also applicable to the case where the anode is in the plane $z=-c$ ($\zeta=-1$) and the cathode is in the plane $z=+c$ ($\zeta=+1$). In the latter situation, the reference fields V_0, j_0, and E_0 [Eqs. (4),(51)] are positive, since $I>0$. These explanations hold for magnetic fields pointing in the positive z direction, $B_0>0$; V_0 changes its sign with the sign of B_0 [Eq. (4)]. Note that the magnetic Reynolds number R in Eq. (11) is defined to change its sign with the sign of V_0.

III. APPLICATIONS

As an illustration, the radial (ρ) dependence of the dimensionless discharge fields $V(\rho,\zeta)$, $B(\rho,\zeta)$, $E_\rho(\rho,\zeta)$, $J_\rho(\rho,\zeta)$, and $J_\zeta(\rho,\zeta)$ has been computed for $I<0$ in the cross-sectional planes $\zeta=-0.99$ (cathode region), $\zeta=0$ (central region), and $\zeta=+0.99$ (anode region) based on Eqs. (46)–(50). The remaining field $E_\zeta(\rho,\zeta)$ is proportional to $J_\zeta(\rho,\zeta)$ [Eq. (50)]. The characteristic (dimensionless) magnetic interaction number H is treated as a parameter: $H=1$, 10, 100. The geometry parameter $N=c/R_0$ is taken to be $N=1$ corresponding to $R_0=c$ [Eq. (11)]. The radial positions of the cathode and anode are assumed to be

$$\rho_-=0.01\ \ (R_-=0.01R_0),\ \rho_+=0.9\ \ (R_+=0.9R_0).$$

With the exception of $B_\theta=B_0B$, the dimensional fields are negative everywhere where the dimensionless fields are positive, and vice versa since $V_0<0$, $j_0<0$, and $E_0<0$ for $I<0$ [Eqs. (4),(51)].

The Eqs. (46)–(50) indicate that the velocity field $V(\rho,\zeta)$, the current density field $J_{\rho,\zeta}(\rho,\zeta)$, and the electric field $E_{\rho,\zeta}(\rho,\zeta)$ are independent of the magnetic Reynolds number R, whereas the induced magnetic field $B(\rho,\zeta)$ is proportional to R. This is due to the azimuthal direction of the induced magnetic field $B(\rho,\zeta)$, which is parallel to the velocity field $V(\rho,\zeta)$ of rotation. Accordingly, the plasma fields $V(\rho,\zeta)$, $B(\rho,\zeta)/R$, $J_{\rho,\zeta}(\rho,\zeta)$, and $E_{\rho,\zeta}(\rho,\zeta)$ depend only on the Hartmann number H, presuming that the Hall effect is negligible ($\omega\tau\ll1$).

Central region, $\zeta=0$. In Figs. 2–6, $V(\rho,0)$, $[B(\rho,0)-R\rho]/R$, $E_\rho(\rho,0)$, $J_\rho(\rho,0)$, and $J_\zeta(\rho,0)\propto E_\zeta(\rho,0)$ are shown versus $0\leq\rho\leq1$ with $H=1$, 10, 100 as a parameter. It is seen that $|V|$ increases considerably at any point $0<\rho<1$ as H is increased. Similarly, $(B-R\rho)/R$ and the sources $J_{\rho,\zeta}$ of the magnetic induction increase in intensity within the main central region $0<\rho<1-\Delta\rho$ as H is increased. For large values $H\gtrsim10$, B and $J_{\rho,\zeta}$ decrease in the wall region $\Delta\rho=\Delta\rho(H)$, so that the electrical discharge becomes more concentrated in the center $0<\rho<1-\Delta\rho$ of the centrifuge. The intensity of E_ρ increases uniformly in the region $0<\rho<1$ as H is increased, while $E_\zeta\propto J_\zeta$.

Cathode region, $\zeta=-0.99$. The Figs. 7–11 show $V(\rho,-0.99)$, $[B(\rho,-0.99)-R\rho]/R$, $E_\rho(\rho,-0.99)$, $J_\rho(\rho,-0.99)$, and $J_\zeta(\rho,-0.99)\propto E_\zeta(\rho,-0.99)$ versus $0\leq\rho\leq1$ for $H=1$, 10, 100. The fields V, $E_{\rho,\zeta}$, and $J_{\rho,\zeta}$ increase in intensity at any point $0<\rho<1$ with increasing H, whereas B/R decreases in $0<\rho<1$ with increasing H. Since the ring cathode is at $\rho_-=0.01$ ($\zeta=-1$), the field distributions are more closely concentrated at the axis $\rho\cong0$ than those in the plane $\zeta=0$ (Figs. 2–6). Note that the plasma rotates only in the region $\rho\cong0.1$ with a significant velocity, since the Lorentz force $-j_rB_0$ decreases

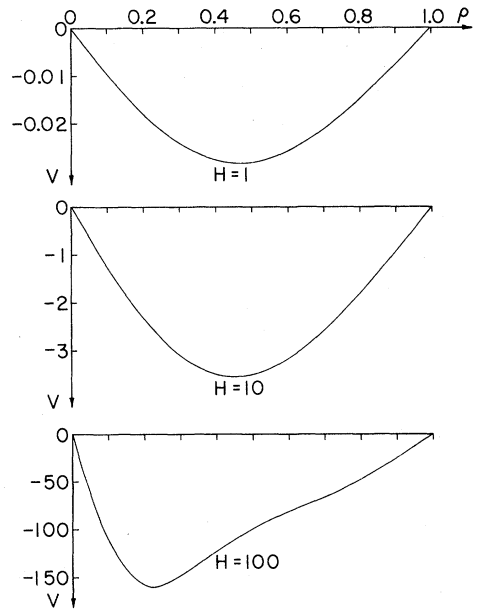

FIG. 2. $V(\rho,\zeta)$ versus ρ for $\zeta=0$, and $H=1,10,100$.

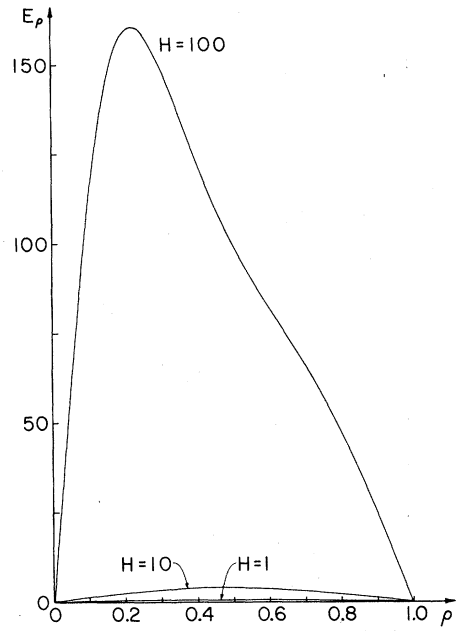

FIG. 4. $E_\rho(\rho,\zeta)$ versus ρ for $\zeta=0$, and $H=1,10,100$.

rapidly with increasing $\rho\to 1$.

Anode region, $\zeta=+0.99$. The Figs. 12–16 present $V(\rho,+0.99)$, $[B(\rho,+0.99)-R\rho]/R$, $E_\rho(\rho,+0.99)$, $J_\rho(\rho,+0.99)$, $J_\zeta(\rho,+0.99)\propto E_\zeta(\rho,+0.99)$ versus $0\leq\rho\leq 1$ for $H=1$, 10, 100. The velocity field is fully developed nearly through the entire centrifuge cross section $0<\rho\lesssim 0.9$, since the Lorentz force $-j_r B_0$ is strongest in the vicinity $\rho\cong 0.9$ of the ring anode $\rho=0.9$ ($\zeta=+1$). As a result, a thin and steep boundary layer exists close to the cylinder wall ($\rho=1$) with plasma counter-rotation at sufficiently small H values. The radial distributions of $B, E_{\rho,\zeta}, J_{\rho,\zeta}$ clearly indicate that, in the plane $\zeta=+0.99$, the electrical discharge has shifted to the region $\rho\cong 0.9$ due to the influence of the (nearby) ring anode at $\rho=0.9$ ($\zeta=+1$).

In the graphical illustrations, the cathode radius R_- was chosen to be small compared to the anode radius R_+ to ensure a large angle between the current field lines $\vec{j}(\vec{r})$ and the external magnetic field

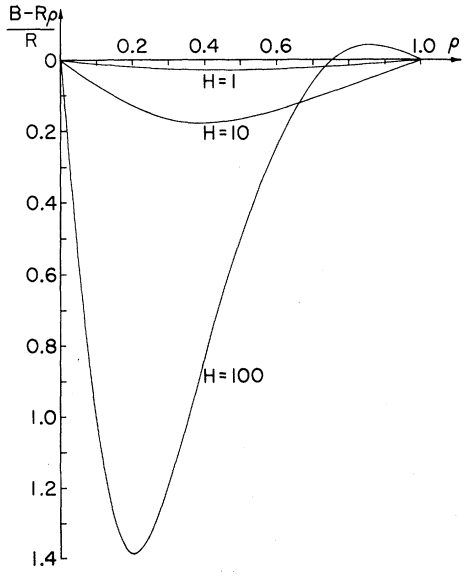

FIG. 3. $[B(\rho,\zeta)-R\rho]/R$ versus ρ for $\zeta=0$, and $H=1$, 10, 100.

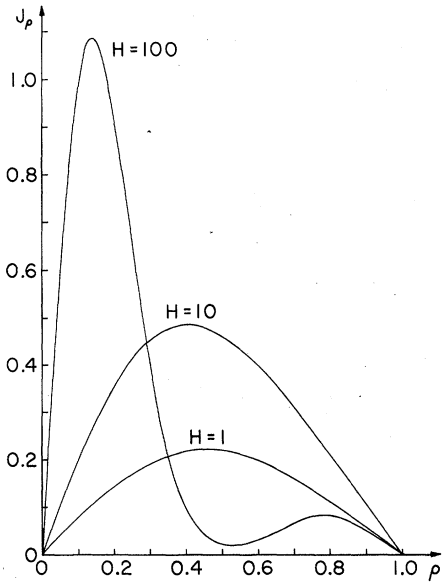

FIG. 5. $J_\rho(\rho,\zeta)$ versus ρ for $\zeta=0$, and $H=1,10,100$.

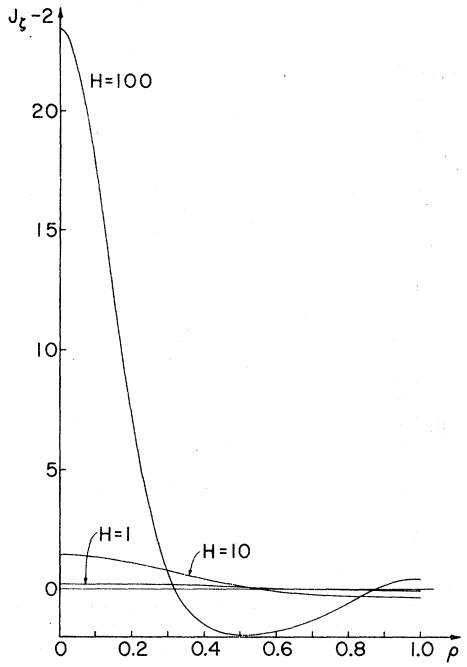

FIG. 6. $J_\zeta(\rho,\zeta)-2$ versus ρ for $\zeta=0$, and $H=1,10,100$.

$\vec{B}_0$, i.e., a significant Lorentz force. A comparison of the Figs. 2 and 7 with Fig. 12 indicates that this choice of electrode radii results in a radial boundary layer of large width and low velocity in the lower half $-c \leq z \lesssim 0$ of the centrifuge. Hence, $R_- \ll R_+$ (or $R_- \gg R_+$) is not the best choice for a centrifuge of maximum efficiency. Figure 12 demonstrates that a velocity profile rising uniformly with radius r and decreasing rapidly in a steep boundary layer of narrow width Δr, is obtained by using a cathode and an anode of the same radius $R_- = R_+ \lesssim R_0$, which is nearly as large as the centrifuge radius R_0. Although $R_- = R_+$ in this case, the current field lines $\vec{j}(\vec{r})$ intersect with $\vec{B}_0$ at a sufficiently large angle due to the repulsion of the current filaments. As a result, a net Lorentz torque results for a

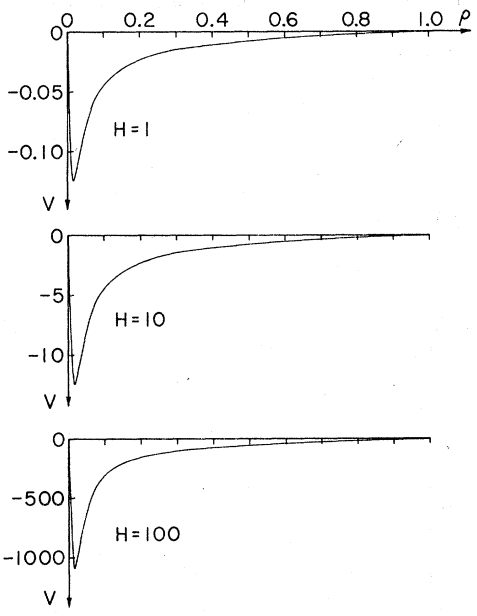

FIG. 7. $V(\rho,\zeta)$ versus ρ for $\zeta=-0.99$, and $H=1,10,100$.

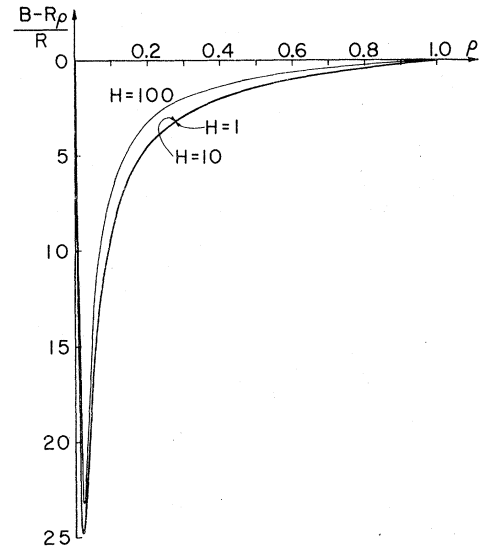

FIG. 8. $[B(\rho,\zeta)-R\rho]/R$ versus ρ for $\zeta=-0.99$, and $H=1,10,100$.

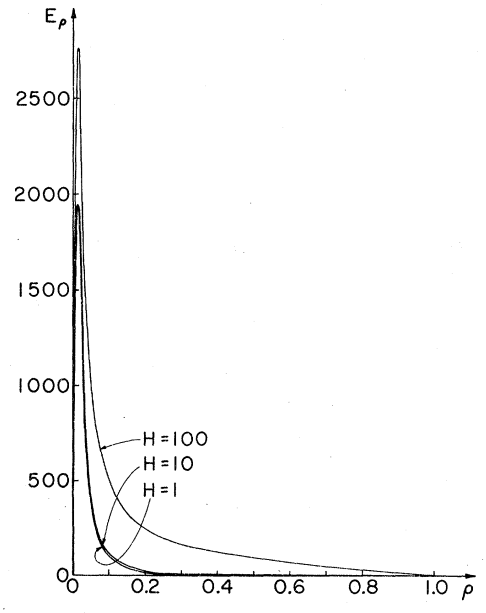

FIG. 9. $E_\rho(\rho,\zeta)$ versus ρ for $\zeta=-0.99$, and $H=1,10,100$.

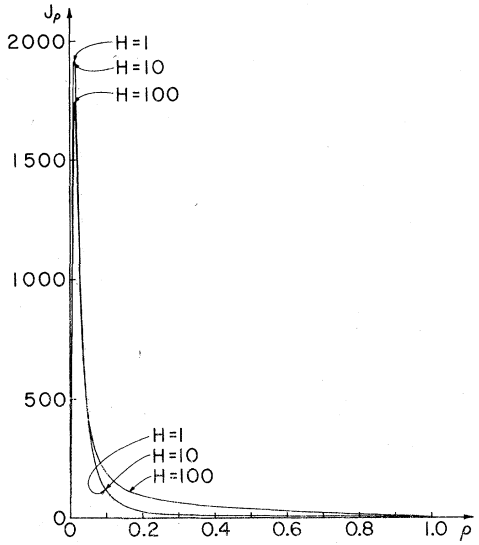

FIG. 10. $J_\rho(\rho,\zeta)$ versus ρ for $\zeta=-0.99$, and $H=1, 10, 100$.

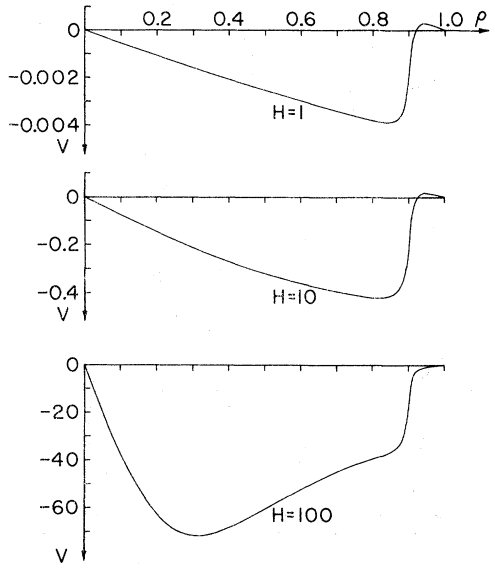

FIG. 12. $V(\rho,\zeta)$ versus ρ for $\zeta=+0.99$, and $H=1, 10, 100$.

centrifuge with $R_-=R_+$ which is still of the same order of magnitude as for a centrifuge with $R_-\ll R_+$ (presuming that I, and B_0, c, and R_0 are the same).

The Figs. 2–16 are based on the Fourier series solutions, which were summed numerically up to $n=100$, and the eigenvalues k_n, $n=1,2,3,\ldots 100$, were computed up to the tenth decimal point. The resulting accuracy is adequate as a test run with $n=110$ indicated.

The centrifuge analysis presented indicates that extremely high speeds of plasma rotation are obtainable at moderate discharge currents I and magnetic inductions B_0, presuming the Hartmann number H is not small, $H>1$. As an example, consider an isotope centrifuge discharge with:

$$|I| = 10^2 \text{ amp}, \quad |B_0| = 10^0 \text{ T},$$

$$\sigma = 10^2 \text{ mho m}^{-1}, \quad R_0 = c = 10^{-1} \text{ m}.$$

Hence, by Eq. (14)

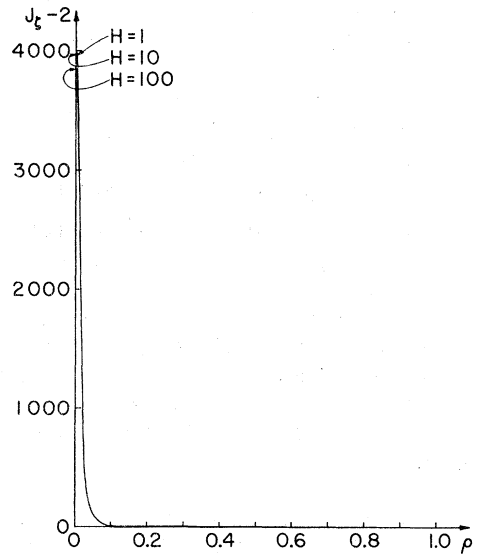

FIG. 11. $J_\zeta(\rho,\zeta)-2$ versus ρ for $\zeta=-0.99$, and $H=1, 10, 100$.

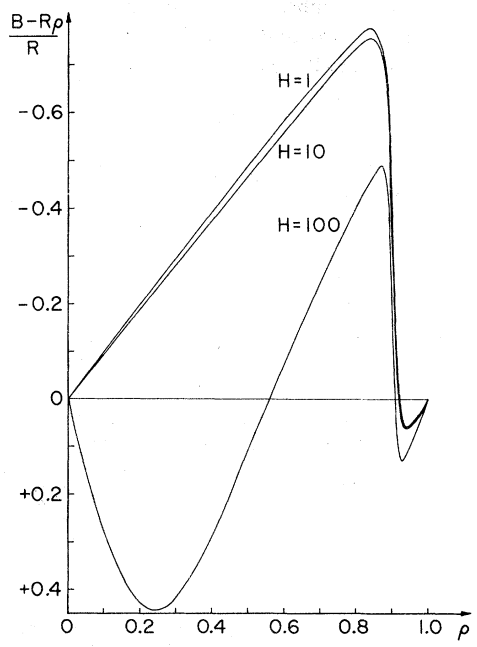

FIG. 13. $[B(\rho,\zeta)-R\rho]/R$ versus ρ for $\zeta=+0.99$, and $H=1, 10, 100$.

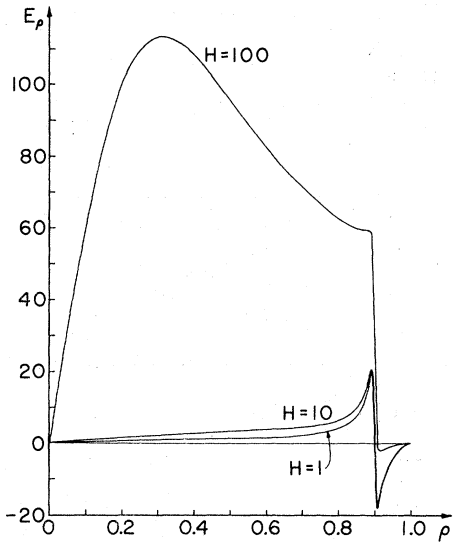

FIG. 14. $E_\rho(\rho,\zeta)$ versus ρ for $\zeta=+0.99$, and $H=1, 10, 100$.

$$V_0 = I/2\pi R_0 B_0 \sigma c = (5/\pi)\times 10^1 \text{ m sec}^{-1},$$

and, by Fig. 2,

$$V_\theta = V_0 V \sim 10^3 \text{ m sec}^{-1}, \quad \text{for } H=100.$$

Since the working gas of the centrifuge discharge consists of two isotope gases, the centrifugal forces would concentrate the lighter isotope ions and atoms in the central region and enrich the heavier isotope atoms and ions in the peripheral region of the discharge. According to the equations of motion for two isotopes of masses m_i and m_j, the isotope density ratio at distances $0<r<R_0-\Delta r$,

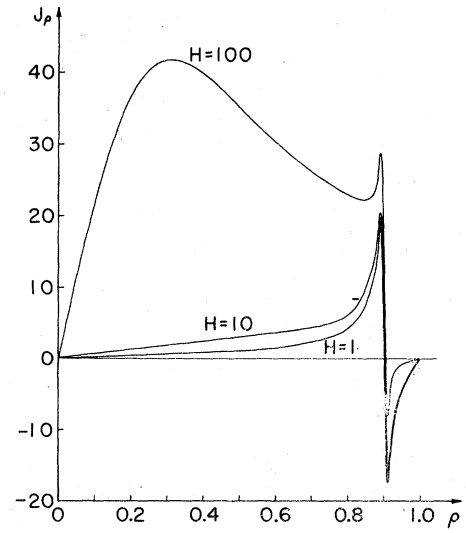

FIG. 15. $J_\rho(\rho,\zeta)$ versus ρ for $\zeta=+0.99$, and $H=1, 10, 100$.

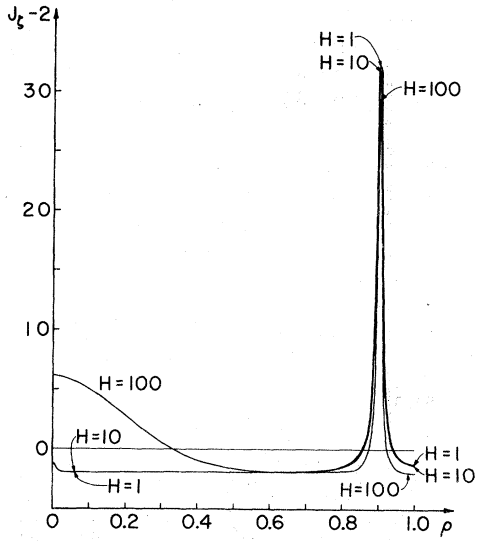

FIG. 16. $J_\zeta(\rho,\zeta)-2$ versus ρ for $\zeta=+0.99$, and $H=1, 10, 100$.

where Δr is the viscous boundary layer thickness, is approximately (T_0 is the temperature of the isotope ions)

$$\frac{\bar{n}_i(r)}{\bar{n}_j(r)} \cong \frac{\bar{n}_i(0)}{\bar{n}_j(0)} \exp\left(+\frac{\frac{1}{2}\Delta m_{ij}\bar{V}_\theta(r)^2}{kT_0}\right), \quad \Delta m_{ij} = m_i - m_j,$$

where the bar designates a spatial average over the region $|z|<c$.

As a specific example, consider a uranium plasma centrifuge containing the isotope ions $(i)U^{237}$ and $(j)U^{235}$ at a temperature $T_0 = 10^3$ °K (and electrons at a temperature $T_e > T_0$). In this case, one has $\Delta m_{ij} = m(237) - m(235) = 3.320\times 10^{-27}$ kg, $kT = 1.381\times 10^{-20}$ J. Hence, the isotope separation ratio is:

$$\frac{\bar{n}_{237}(r)/\bar{n}_{235}(r)}{\bar{n}_{237}(0)/\bar{n}_{235}(0)}$$

$$\cong 1.128\times 10^0 \quad \text{for } \bar{V}_\theta(r) = 1\times 10^3 \text{ m sec}^{-1}$$

$$\cong 1.617\times 10^0 \quad \text{for } \bar{V}_\theta(r) = 2\times 10^3 \text{ m sec}^{-1}$$

$$\cong 2.950\times 10^0 \quad \text{for } \bar{V}_\theta(r) = 3\times 10^3 \text{ m sec}^{-1}.$$

Based on these examples, one can assume with some confidence that high-power plasma centrifuges are technically realizable employing dense, collision-dominated isotope plasmas. The separation of isotopes by centrifugal forces in low density plasmas has been established experimentally.[10,11,20-24]

A disadvantage of collisionless plasma centrifuges is the small amount of isotopes they permit to separate. The proposed high-density plasma centrifuge would use arc plasmas at pres-

sures of about one atmosphere so that the isotope masses separated are increased by orders of magnitude. The large Hartmann numbers $H = (\sigma/\mu)^{1/2} B_0 R_0$ required for high speeds of isotope rotation are achievable because of the (relative) small viscosity μ and large conductivity σ of gaseous plasmas. Speeds of plasma rotation, which are an order-of-magnitude larger than those in the above examples, can be achieved at realistic Hartmann numbers H. Since $\omega = 1.76 \times 10^{11} B$ sec, the Hall effect is insignificant in dense plasmas for $B = 1$ T as long as $\tau < 10^{-12}$ sec. In general, the Hall effect increases the speed of plasma rotation for $\omega\tau > 1$, i.e., in plasmas of lower density.[29] In developing a plasma centrifuge, therefore, apparently a trade-off between isotope density and rotation velocity has to be made.

For mathematical convenience, we have disregarded possible secondary flows (superimposed on the main azimuthal flow) in the analysis of the plasma centrifuge. Although experiments indicate secondary flows in the motion of liquids between rotating cylinders,[30] secondary flows have apparently not been observed in plasmas which rotate under the influence of electromagnetic forces. In spite of the mathematical complications involved, consideration of secondary flows would be of interest from the theoretical point of view.

---

*Supported in part by NASA.

[1]G. Lehner, *Reactions under Plasma Conditions*, edited by M. Venugopalan (Wiley-Interscience, New York, 1971).
[2]N. N. Komarov and V. M. Fadeev, Zh. Eksp. Teor. Fiz. 41, 528 (1961) [Sov. Phys. JETP 14, 378 (1962)].
[3]M. V. Samakhin, Dokl. Akad. Nauk SSSR, Fiz. 155, 72 (1964).
[4]E. M. Dobryshevskii, Zh. Tekh. Fiz. 33, 1210 (1963) [Sov. Phys. Tech. Phys. 8, 903 (1964)].
[5]B. Bonnevier and B. Lehnert, Ark. Fys. 16, 231 (1959).
[6]J. Bergstroem, S. Holmberg, and B. Lehnert, Ark. Fys. 23, 543 (1962).
[7]J. Bergstroem, S. Holmberg, and B. Lehnert, Ark. Fys. 25, 49 (1963).
[8]B. Lehnert, Ark. Fys. 28, 205 (1964).
[9]B. Lehnert, Y. Bergstroem, and S. Holmberg, Nucl. Fusion 6, 231 (1966).
[10]B. Bonnevier, Ark. Fys. 33, 255 (1966).
[11]B. Bonnevier, Plasma Phys. 13, 763 (1970).
[12]B. Lehnert, Phys. Scr. 2, 106 (1970).
[13]B. Lehnert, Nucl. Fusion 11, 485 (1971).
[14]B. Lehnert, Phys. Scr. 7, 102 (1973).
[15]B. Lehnert, Phys. Scr. 9, 229 (1974).
[16]E. A. Witalis, Plasma Phys. 10, 747 (1968).
[17]E. A. Witalis, Z. Naturforsch. 29a, 1138 (1974).
[18]H. Mahn, H. Ringler, and G. Zankel, Z. Naturforsch. 23a, 868 (1968).
[19]R. Schwenn, Z. Naturforsch. 25a, 1601 (1970).
[20]J. C. Guilloud, Entropie 34, 23 (1970).
[21]H. Heller and M. Simon, Phys. Lett. 50 A, 139 (1974).
[22]B. N. James and S. W. Simpson, Phys. Lett. 64 A, 347 (1974).
[23]T. Ban and T. Sekiguchi, Jpn. J. Appl. Phys. 14, 1411 (1975).
[24]T. Ban and T. Sekiguchi, Jpn. J. Appl. Phys. 15, 115 (1976).
[25]C. C. Chang and T. S. Lundgren, Phys. Fluids 2, 627 (1959).
[26]O. Okada and T. Dodo, J. Nucl. Sci. Technol. 10, 626 (1973).
[27]L. E. Kalikhman, *Magnetogasdynamics* (Saunders, Philadelphia, 1967).
[28]G. P. Tolstov, *Fourier Series* (Prentice-Hall, Englewood-Cliffs, N. J., 1962).
[29]H. E. Wilhelm and S. H. Hong, J. Appl. Phys. 48, 561 (1977).
[30]H. Schlichting, *Boundary-Layer Theory* (McGraw-Hill, New York, 1968).